ELSEVIER

www.elsevier.nl/locate/jorganchem

Journal of Organometallic Chemistry 598 (2000) 42–48

Journal of Organometallic Chemistry

Synthesis and properties of some novel ferrocene macrocyclic dioxopolyamines

Peng Xue, Enqin Fu *, Guochao Wang, Cuiqin Gao, Maohai Fang, Chengtai Wu

Department of Chemistry, Wuhan University, Wuhan 430072, People's Republic of China

Received 5 August 1999; received in revised form 25 October 1999

Abstract

A series of novel ferrocene macrocyclic dioxopolyamines (**1**–**4**) bearing an iminodiacetamide fragment in their framework were designed and synthesized, and two such new ligands (**2** and **4**) and some of their complexes are reported. The coordination behavior and electrochemical properties of these compounds were systematically examined by cyclic voltammetry (CV) and electronic absorption spectroscopy. Host–guest complexation stoichiometries (1:1) have been confirmed by fast atom bombardment mass spectroscopy (FAB MS) and UV–vis titration of cobalt ion and ligands **3** and **4**. Additionally the stability constants for the equilibrium of cobalt ion and ligands **3** and **4** have been evaluated. The coordination of the ligands with transition metal ions (Cu^{2+}, Ni^{2+} and Co^{2+}) causes anodic shifts of the ferrocene redox couple to various extents. The uncommon oxidation state of nickel(III) and copper(III) can be selectively stabilized by tetra-azamacrocycle **1** and penta-azamacrocycles, **3** and **4**, respectively.

Keywords: Ferrocene; Macrocyclic dioxopolyamine; Synthesis; Cyclic voltammetry; Coordination; UV–vis spectrometry

1. Introduction

In recent years, studies of redox-active host molecules, especially those containing a ferrocene unit as redox-active center, have attracted much attention for their potential application in fields such as chemical sensors [1–3], redox-switchable ligands [4] and redox catalysts [5]. Ferrocene macrocyclic polyamines have shown some interesting electrochemical behavior. Though it is difficult to synthesize, some compounds of this kind have been reported in the literature [5–7]. Recently we reported the synthesis of two series of ferrocene macrocyclic dioxopolyamines [7]. We choose the dioxopolyamines as the coordination site because of their unique dual structural features of saturated macrocyclic polyamines and oligopeptides, and their interesting coordination behavior [8,9]. These redox-active dioxopolyamines may exhibit some interesting chemical properties and/or biological functions. For example, they may serve as redox enzyme models and be applied in redox catalysis systems and/or used as drugs based on their chemical reactivity [9]. In order to systematically investigate macrocyclic polyamines carrying an iminodiacetamide fragment in their framework, we synthesized two new compounds **2** and **4** on the basis of the previous work [7a]. Some complexes of these ligands were also prepared. In this paper, we report the syntheses, electrochemistry and coordination chemistry of this series of compounds by using cyclic voltammetry (CV) and UV–vis spectrometry.

2. Experimental

2.1. General

Dimethyl ferrocenylmethyliminodiacetate (**5**), 1-ferrocenylmethyl 1,4,7,10-tetraaza-cyclododecane-3,11-dione (**1**) and 1-ferrocenylmethyl-1,4,7,10,13-pentaazacyclopentadecane-3,14-dione (**3**) were prepared according to the method in our previous report [7a], *N*,*N*-bis(2-aminoethyl)-1,3-propylenediamine (**6**) [10] was prepared according to a procedure in the literature, and

* Corresponding author. Tel.: +86-27-87684117; fax: 86-27-87647617.

E-mail address: jgqin@whu.edu.cn (E. Fu)

0022-328X/00/$ - see front matter
PII: S0022-328X(99)00668-3

the other polyamines were commercially available and distilled before use. The solvents used for the reaction were thoroughly dried analytical reagents. All melting points were uncorrected. IR spectra were obtained on a Nicolet 170SX FTIR spectrophotometer. Proton magnetic resonance spectra (300 MHz) and ^{13}C magnetic resonance spectra (75 MHz) were recorded on a Varian 300 spectrometer with TMS as internal reference. Fast atom bombardment mass spectra (FAB MS) were recorded on a ZAB 3F-HF spectrometer.

CV was performed in a conventional three-electrode cell at 20 ± 1°C, using a Princeton Applied Research model 173 potentiostat–galvanostat (EG&G), controlled by a personal computer installed with the M352 system, the working electrode was glassy carbon (area = 0.126 cm^2), a platinum coil was used as the counter-electrode and a saturated calomel electrode (SCE) was used as the reference electrode. All the experiments were done at a scan rate of 30 mV s^{-1} in 0–0.8 V. A mixture of 95% EtOH–H_2O (double-distilled) (2:1 v/v) was employed as solvent using $NaClO_4$ (0.1 mol dm^{-3}) as the supporting electrolyte. The aqueous solutions of the metal cations (0.1 mol dm^{-3}) were prepared from their sulfate of nitrate (all are analytical reagents). All the tested ligands were 1 mmol dm^{-3} in concentration. The electrochemical solutions were bubbled with nitrogen before each experimental and throughout the investigation.

UV–visible spectra were recorded on a Shimadzu UV-160A recording spectrometer at 20 ± 1°C in a 1 : 1(v/v) EtOH–H_2O solution unless otherwise stated, the ligands were all 2.0 mmol dm^{-3} in concentration except in the titration of the ligand **3** (1 mmol dm^{-3}) with cobalt(II). The transition metal salts were used as described in electrochemical experiments. After addition of metal ions, the solutions of the ligands were adjusted to ca. pH 7 with NaOH (0.01 mol dm^{-3}) except in the titration experiments (ca. pH 6).

2.2. Synthesis of the ligands

2.2.1. 1-Ferrocenylmethyl-1,4,8,12-tetraaza-cyclotetradecane-3,13-dione (2)

Dimethyl ferrocenylmethyliminodiacetate (**5**) (3.59 g 10.0 mmol) and 1,5,9-triazanonane (**7**) (1.31 g, 10.0 mmol) were dissolved in dry methanol (50 ml), respectively, and the solutions were simultaneously added to dry methanol (300 ml) with stirring, the resulting solution was heated to reflux under nitrogen for 10 days. After the solvent was removed in vacuum, the product was separated by column chromatography on alumina (100:2 $CHCl_3$–MeOH, v/v) and the compound was obtained as a yellow powder. Yield: 0.51 g (12%), m.p. 166–168°C. FAB MS (exact mass, 426.17; *m/z*, %): 427 ($M^+ + 1$, 10); 426 (M^+, 20); 361 ($M - 65$, 9); 283 ($M - 199 + Fe$, 18); 199 ($C_5H_5FeC_5H_4CH_2^+$, 100). ^1H-NMR ($CDCl_3$) δ (ppm): 0.80 (1H, br, s, C–NH–C); 1.65 (4H, br, s, CCH_2C); 2.74 (4H, br, s, CH_2NCH_2); 3.16 (4H, s, NCH_2CO); 3.29 ~ 3.34 (4H, m, $CONCH_2$); 3.42 (2H, s, $FcCH_2$); 4.09 (s), 4.10 ~ 4.12 (q) (9H, ferrocenyl); 8.20 (2H, br, s, CONH). ^{13}C-NMR ($CDCl_3$) δ (ppm): 28.2 (C–CH_2–C); 40.9 (CONH–CH_2); 52.5 (CH_2NCH_2); 56.6, 60.9 (NCH_2CO, $FcCH_2$); 68.77, 68.84, 69.95 (C–H, of ferrocenyl); 82.4 (1-C, of ferrocenyl); 170.3 (C=O). IR (cm^{-1}, KBr pellet): 3331 (N–H, CONH); 3096 (C–H, of ferrocenyl); 2919, 2845 (C–H, of alkyl); 1661 (C=O, CONH); 1107, 1027, 816 (m-s, of ferrocenyl). Anal. Calc. for $C_{21}H_{30}N_4O_2Fe$: C, 59.2; H, 7.1; N, 13.1. Found: C, 58.8; H, 7.0; N, 12.9%.

2.2.2. 1-Fererocenylmethyl-1,4,7,11,14-pentaaza-cyclohexadecane-3,15-dione (4)

This compound was prepared following the same procedure as described for **2** except that refluxing was carried out for 15 days. After column chromatography on alumina (100:3 $CHCl_3$–MeOH, v/v), recrystallization from acetone yielded yellow needles. Yield 0.80 g (18%), m.p.162–163°C. FAB MS (exact mass, 455.20; *m/z*, %): 456 ($M^+ + 1$, 20); 455 (M^+, 15); 390 ($M - 65$,3); 312 ($M - 199 + Fe$,11); 199 (C_5H_5Fe–$C_5H_4CH_2^+$, 100). ^1H-NMR ($CDCl_3$) δ (ppm): 1.72–1.74 (2H, m, CCH_2C); 1.85 (2H, br, CNHC); 2.70–2.75 (8H, m, CH_2NCH_2); 3.15 (4H, s, NCH_2CO); 3.34–3.35 (4H, br, m, $CONCH_2$); 3.44 (2H, s, $FcCH_2$); 4.09, 4.13 (9H, s, s, ferrocenyl); 7.12 (2H, br, s, CONH). ^{13}C-NMR ($CDCl_3$) δ (ppm): 29.7 (C–CH_2–C); 38.6 (CONH–CH_2); 49.6, 49.9 (CH_2NCH_2); 56.5, 60.1 (NCH_2CO, $FcCH_2$); 68.86, 68.93, 69.98 (C–H, of ferrocenyl); 81.8 (1-C, of ferrocenyl); 170.0 (C=O). IR (cm^{-1}, KBr pellet): 3318 (N–H, CONH); 3096 (C–H, of ferrocenyl); 2924, 2873 (C–H, of alkyl); 1661 (C=O, CONH); 1105, 1028, 820 (m-s, of ferrocenyl). Anal. Calc. for $C_{22}H_{33}N_5O_2Fe$: C, 58.0; H, 7.3; N, 15.4. Found: C, 58.2; H, 7.2; N, 15.3%.

2.3. Preparation of the complexes

2.3.1. Copper(II) complex of 1, [CuH_2L(1)]

The ethanol solution (20 ml) of **1** (0.199 g, 0.5 mmol) and $Cu(OAc)_2 \cdot H_2O$ (0.100 g, 0.5 mmol) was heated to reflux under nitrogen for 2 h. After the solvent was removed in vacuum, recrystallization from acetonitrile–acetone yielded green needles. FAB MS (exact mass, 459.06; *m/z*, %): 460 ($M^+ + 1$,24); 459 (M^+, 18); 398 ($(1)^+$, 3); 261 (M-199, 10); 197 ($M - 199 - 64$, 8); 199 ($C_5H_5FeC_5H_4$–CH_2^+, 100). IR (cm^{-1}, KBr pellet): 3094 (C–H, of ferrocenyl); 2929 (C–H, of alkyl); 1598 (C=O, CON^-); 1104, 1025, 820 (m-s, of ferrocenyl). UV–vis (λ_{max}, nm; (ε, dm^3 mol^{-1} cm^{-1})): 419 (168), 550 (137). Anal. Calc. for $C_{19}H_{24}CuFeN_4O_2$: C, 49.6; H, 5.3; N, 12.2. Found: C, 49.1; H, 5.3; N, 12.1%.

*2.3.2. Nickel(II) complex of **1**, [NiH$_{-2}$L(1)]*

This complex was obtained following the same procedure described for [CuH$_{-2}$L(**1**)]. Recrystallization from acetonitrile–ethanol yielded pale green needles. FAB MS (exact mass, 454.06; *m*/*z*, %): 455 ($M^+ + 1$, 30); 454 (M^+, 8); 398 ($(1)^+$, 2); 255 (M − 199 − 1, 7); 197 (M − 199 − 59, 8); 199 ($C_5H_5FeC_5H_4CH_2^+$, 100). IR (cm^{-1}, KBr pellet): 3078 (C–H, of ferrocenyl); 2953 (C–H, of alkyl); 1557 (C=O, CON^-); 1105, 1001, 823 (m-s, of ferrocenyl). UV–vis (λ_{max}, nm; (ε, $dm^3\ mol^{-1}\ cm^{-1}$)): 428 (147), 325 (232). Anal. Calc. for $C_{19}H_{24}FeN_4NiO_2$: C, 50.2; H, 5.3; N, 12.3. Found: C, 49.1; H, 5.4; N, 12.3%.

*2.3.3. Copper(II) complex of **3**, [CuH$_{-2}$L(**3**)]*

This complex was obtained following the same procedure described for [CuH$_{-2}$L(**1**)]. Recrystallization from acetone–H_2O yielded a black–green powder. FAB MS (exact mass, 502.11; *m*/*z* %): 503 ($M^+ + 1$, 19); 502 (M^+, 19); 199 ($C_5H_5FeC_5H_4CH_2^+$, 100). IR (cm^{-1}, KBr pellet): 3096 (C–H, of ferrocenyl); 2913, 2861 (C–H, of alkyl); 1603 (C=O, CON^-); 1104, 1005, 823 (m-s, of ferrocenyl). UV–vis (λ_{max}, nm; (ε, $mol^{-1}\ dm^3\ cm^{-1}$)): 401 (220), 556 (135); 410 (247), 598 (135), in 95% EtOH. Anal. Calc. for $C_{21}H_{29}CuFeN_5O_2$: C, 50.2; H, 5.8, N, 13.9. Found: C, 50.1; H, 5.8; N, 13.7%.

*2.3.4. Cobalt(II) complex of **3**, [CoH$_{-2}$L(**3**)]*

This complex was obtained following the same procedure described for [CuH$_{-2}$L(**1**)]. Recrystallization from ethanol yielded a dark red powder. FAB MS (exact mass, 498.10, *m*/*z*, %): 499 ($M^+ + 1$, 7); 498 (M^+, 19); 497 ($M^+ - 1$, 20); 199 ($C_5H_5FeC_5H_4CH_2^+$, 100). IR (cm^{-1}, KBr pellet): 3075 (C–H, of ferrocenyl); 2928, 2880 (C–H, of alkyl); 1605 (C=O, CON^-); 1101, 1005, 818 (m-s, of ferrocenyl). UV–vis (λ_{max}, nm; ($\varepsilon\ mol^{-1}\ dm^3\ cm^{-1}$)): 362 (796), 507 (394). Anal. Calc. for $C_{21}H_{29}CoFeN_5O_2$: C, 50.6; H, 5.9; N, 14.1. Found: C, 50.2; H, 6.0; N, 13.9%.

3. Results and discussion

Compounds **1**–**4** were prepared following the procedure shown in Scheme 1:

*3.1. Coordination of compound **1**–**4** with Ni^{2+}, Cu^{2+}, and Co^{2+} ions*

IR, UV–vis spectra and FAB MS data of all the prepared complexes confirmed the complexation between cations and macrocyclic ligands. Their IR spectra showed changes [11a] in stretching vibrations of both C=O (i.e. from ca. 1660 to ca. 1600 cm^{-1}) and N–H (disappeared in the complexes) in amides. FAB MS also showed the molecular ion peaks of MH$_{-2}$L. All attempts to obtain a pure solid-state nickel(II) complex of **3** were unsuccessful.

The shifts in λ_{max} (Table 1) of ferrocene and guest cations were caused by addition of metal ions (1:1, M^{2+}:L, mol/mol) such as Cu^{2+} and Co^{2+} to the solutions of ligand **1**–**4**, but addition of Ni^{2+} caused shifts of only a few nanometers. However, the fact common to all the cases was that there were some changes in the absorbance when the guest cations were added to the solutions of these ligands (for example, see Fig. 1).

The increase in absorbance at λ_{max} for the cobalt complexes of ligands **3** and **4** upon incremental addition of Co^{2+} in air were given in Table 2, the data were illustrated in Fig. 2. The progressive increase in absorbance intercepted in the limiting 'infinity' absorbance at molar ratios of 1.1:1, 0.8:1 of Co^{2+} to the ligands **3** and **4**, respectively. Therefore the complexation stoichiometry for the complexes are both 1:1, which was in agreement with the FAB MS result for the cobalt(II) complex of ligand **3**, although we did not determine the oxidation state of cobalt, the ratio of cobalt to L is the same no matter what oxidation state cobalt is in [9,12]. The equilibrium constants were evaluated by plot of $1/\Delta A$ against 1/[M] based on Benisi–Hildebrand equation [13] to obtain the values for bimolecular equilibrium constants for 2280 (Co^{2+}–**3**), 569 (Co^{2+}–**4**) $mol^{-1}\ dm^3$.

*3.2. Electrochemical behavior of the ligands (**1**–**4**)*

The cyclic voltammograms for ligands before and after addition of Cu^{2+}, Ni^{2+} and Co^{2+} metal ions are showed in Figs. 3–5. The peak potentials (*E* values versus SCE) of each couple are showed in Table 3.

The redox peak separation (70–100 mV) of each complex and ligand (Table 3) indicated the quasi-re-

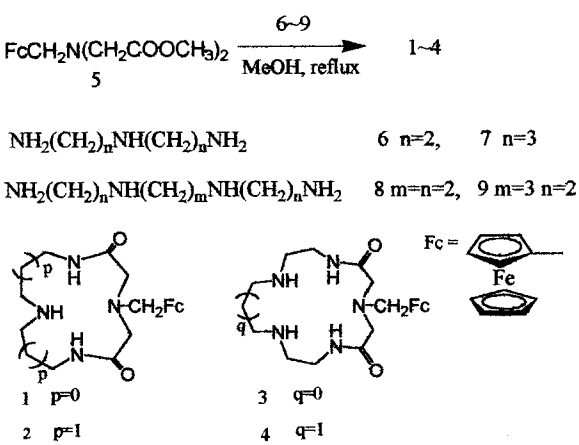

Scheme 1.

Table 1
The values of λ_{max} (nm) and ε (mol^{-1} dm^3 cm^{-1}) for ligands **1**–**4** and their complexes

Complex/ligand		Nil	Co^{2+}	Ni^{2+}	Cu^{2+}
1	λ_1	415	411	415	428
	ε_1	183	157	220	229
	λ_2	315	Nil	317	529 [a]
	ε_2	242	Nil	333	169
2	λ_1	428	408	427	435
	ε_1	143	261	184	139
	λ_2	320	Nil	Nil	Nil
	ε_2	165		Nil	
3	λ_1	414	490 [c]	419	408
	ε_1	195	392	282	270
	λ_2	324 [b]	364	319 [d]	539 [a]
	ε_{20}	360	823	451	148
4	λ_1	428	503 [c]	429	426
	ε_1	154	342	184	204
	λ_2	309	Nil	311	551 [a]
	ε_2	240	Nil	279	154

[a] Copper.
[b] Another at 358 nm (ε, 278).
[c] Cobalt.
[d] Another at 361 nm (ε, 337).

versible redox process for ligands and their complexes except in the case of cobalt(II) complexes **3** and **4**, and the nickel(II) complex of **4**. The bigger values of peak separation might infer stronger electrostatic repulsion between ferrocenium and guest cations (especially in their oxidation state), which caused the cation to move away from the deprotonized amide anions, the reduction peak potentials decreased. On the other hand, the stronger interaction between ferrocene (in **3** and **4**) and guests cations caused the peak potentials increase as described in the following, and as a result the values of the redox peak separation increased. More evidence may come from the irreversible oxidation process and the higher oxidation potential of $Ni^{III/II}$ in the complex of **4** than in that of **3**.

Compared with the free ligands, the addition of transition metal ions has shifted the redox peak potential of the corresponding Fc^+/Fc couple to more anodic position (see Table 3 and the cyclic voltammograms, Figs. 3–5). The ΔE_{pa} values show the difference between the potentials of Fc^+/Fc in the complexed ($E_{pa,c}$) and uncomplexed ($E_{pa,f}$) molecules (Table 3). For those containing smaller ring sizes such as **1** and **2**, the bigger shift (44 and 39 mV, respectively) of oxidation potentials resulted from the addition of the copper(II) ion. On the other hand, for those with bigger ring sizes such as **3** and **4**, the bigger shifts (60, 53 mV, respectively) were obtained upon addition of the cobalt(II) ion. It may be that the metal ionic radii and the coordination configuration of the ligands have an effect on the electrostatic repulsion through space between the ferrocene subunit and the respective metal ion, the stronger the repulsion that exists between them, the bigger shifts caused.

It is interesting to note that a new redox couple [9] ($Cu^{III/II}$, at 644/577 mV) appeared when Cu^{2+} was added into the electrochemical solution of **1** at 0.5, one, and two equivalents (Fig. 3) with the current density increasing slightly until the last addition, but the addition of Ni^{2+} resulted in no new redox couple corresponding to $Ni^{III/II}$. On the other hand, the addition of Ni^{2+} into the electrochemical solutions of **3** and **4**

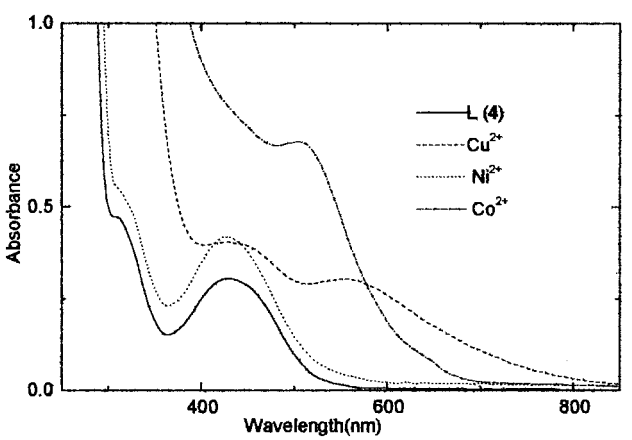

Fig. 1. UV–vis spectra of ligand **4** before and after addition of metal ions.

Table 2
Absorption data at complex λ_{max} for solution of ligand **3** (1 mM) and **4** (2 mM) upon incremental molar ratio addition of Co^{2+}

Co^{2+}:**3**	*A*	Co^{2+}:**3**	*A*	Co^{2+}:**4**	*A*	Co^{2+}:**4**	A
0	0.133	1.125	0.272	0	0.084	0.7875	0.948
0.075	0.158	1.2	0.276	0.0375	0.145	0.8625	0.971
0.15	0.179	1.275	0.279	0.075	0.199	0.9375	0.993
0.3	0.2	1.35	0.283	0.15	0.294	1.0125	1.006
0.375	0.209	1.425	0.288	0.1875	0.34	1.0875	1.021
0.45	0.217	1.5	0.293	0.225	0.377	1.1625	1.032
0.525	0.224	1.575	0.297	0.2625	0.427	1.2375	1.06
0.6	0.234	1.675	0.302	0.3	0.484	1.3125	1.065
0.675	0.243	1.875	0.311	0.3375	0.538	1.3875	1.074
0.75	0.249	2.075	0.315	0.375	0.528	1.4625	1.08
0.825	0.254	2.575	0.321	0.4125	0.577	1.5375	1.083
0.9	0.26	3.075	0.325	0.45	0.657	1.6125	1.097
0.975	0.263	3.575	0.329	0.4875	0.718	1.6875	1.11
1.05	0.268			0.525	0.775	1.7625	1.116
				0.5625	0.838	2	1.125
				0.6375	0.901	2.5	1.156
				0.7125	0.93	3.5	1.233

exhibited new redox peaks [9] (corresponding to $Ni^{III/II}$) at 654/578 mV or 664 mV, respectively (Figs. 4 and 5). The latter was irreversible, although the anodic peak was more marked. The couples existed in the molar ratios 1:0.5, 1:1, 1:2, and the current density (*i*) increased gradually as the concentration of Ni^{2+} increased, except in the case of **3**. However, there was no evidence indicating that the $Cu^{III/II}$ couple appeared in the solutions of **3** and **4** after the addition of the Cu^{2+} ion.

These results suggest that the uncommon oxidation states of Cu^{III} and Ni^{III} can be selectively stabilized by coordination to the corresponding ferrocene macrocyclic dioxopolyamine, namely compound **1** for Cu^{III}, and compound **3** and **4** for Ni^{III}.

The selective stabilization of Cu^{III} and Ni^{III} may be associated with the following aspects: (i) the size of the macrocyclic cavity; (ii) the ionic radii of the two metal ions in different oxidation states; (iii) the coordination configuration, which depends on the ligand-field strength and the electronic states of the metal cations. Due to the strong co-planarity caused by the conjugated imide anions after coordination, the dioxo [12] and N_4 (**1**) yields the square-planar low-spin Ni^{II} complex [9]. The ideal N–M bond length for fitting into the cavity of the coplanar **1** (< 1.83 Å) is not prohibitively short for the low-spin Ni^{II} (Ni^{II}–N average bond length is equal to 1.88–1.89 Å [11a,16a]) [14], but it is too short for the Cu^{II}–N bond length (average value is 1.98–2.00 Å [11b], 2.03 Å [9,16a]), so that the metal ion Cu^{II} has to stay above the coplanar N_4, the change of Cu^{II} to Cu^{III} (d^8, low-spin) will drastically reduce (0.12–0.17 Å) the ionic radius of the metal [15], as a result, Cu^{III} can completely fall into the cavity of the macrocycle and be stabilized. On the other hand, the low-spin d^7 Ni^{III} (Ni^{III}–N bond length is equal to 1.97 Å [16b]) would possess a longer bond length with the N atom than the low-spin d^8 Ni^{II}, the loosely fitting (to Ni^{II}) 15-/16-membered macrocycles **3** and **4** would fit

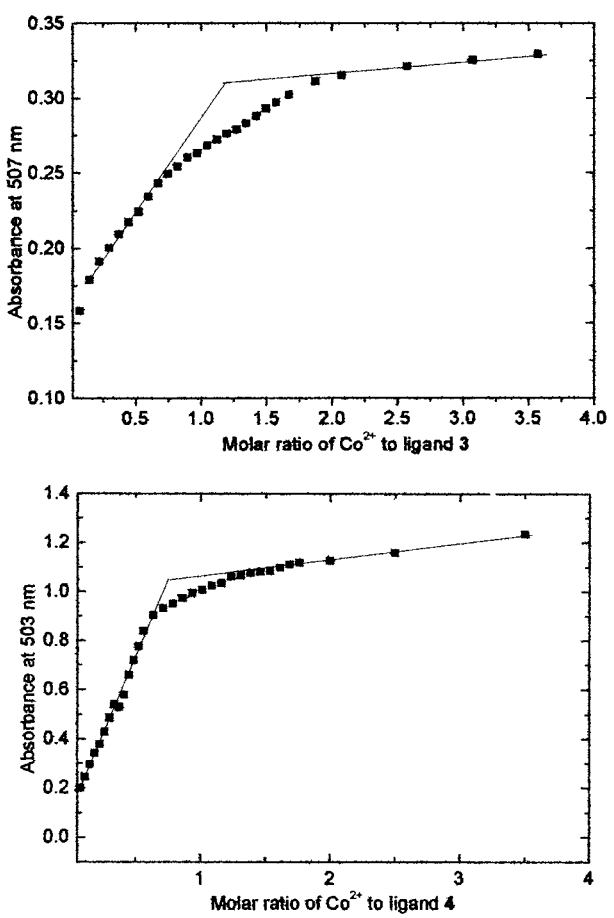

Fig. 2. Plots of A_{max} vs. molar ratio of Co^{2+} to ligand **3** and **4**.

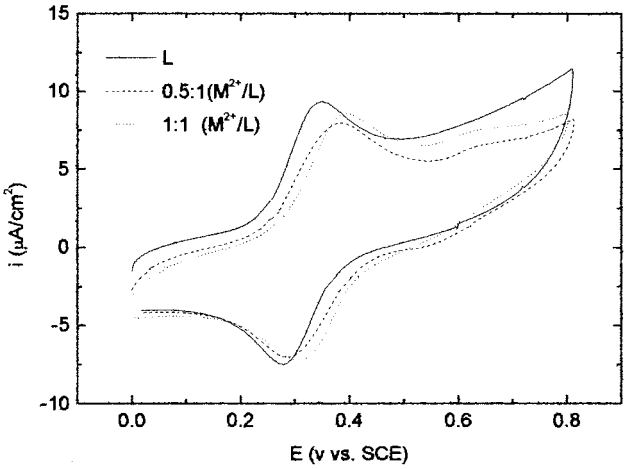

Fig. 3. Cyclic voltammograms of ligand **1** in the presence or absence of Cu^{2+}.

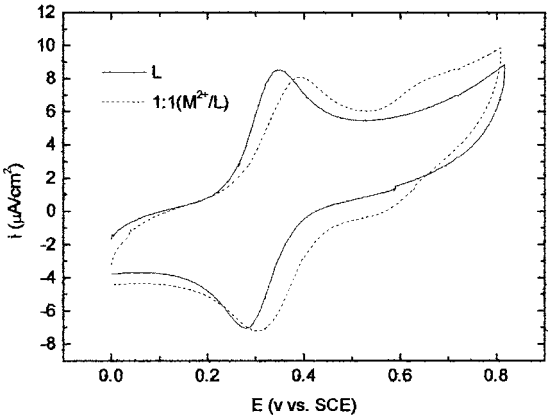

Fig. 4. Cyclic voltammograms of ligand **3** in the presence or absence of Ni^{2+}.

better for Ni^{III}. Moreover, the low-spin d^7 Ni^{III} shows a preference for axial coordination, only the penta-aza-macrocycles **3** and **4** can stabilize the Ni^{III}. As anticipated, **2** showed no evidence for stabilization of either Cu^{III} or Ni^{III}, because it needs a cavity with of smaller size for Cu^{III} and the axial-coordinating atom for Ni^{III}.

Kimura and co-workers [9] have investigated the effect of the cavity size of a series of dioxopolyamines on the stabilization ability of Ni^{III} and Cu^{III}. The trend they found is similar to our work, but the results indicated that our compounds exhibited higher selectivity under our experimental conditions.

Preliminary investigation by CV showed that the E_{pc} value of $Co^{III}L(\mathbf{3})$–O_2 was -370 mV (irreversible) after a solution of the cobalt complex of ligand **3** was kept in air for a few days. However, when the solution was bubbled with nitrogen for 5 min, the peak disappeared. A study of the CoL–O_2 adduct will be the subject of future work.

Table 3
The E values for the compounds **1**–**4** before and after addition of transition metal ions [a]

Complex/ligand		Nil	Co^{2+}	Ni^{2+}	Cu^{2+}
($L:M^{2+}$, mol/mol)		(1:0)	(1:1)	(1:1)	(1:1)
1	E_{pa} (mV)	350	370	357	394 [b], 644 [c]
	E_{pc} (mV)	279	277	271	306 [b], 570 [c]
	ΔE_{pa} (mV) [e]	Nil	20	<10	44
2	E_{pa} (mV)	367	376	376	406
	E_{pc} (mV)	297	296	296	332
	ΔE_{pa} (mV)	Nil	<10	<10	39
3	E_{pa} (mV)	348	408	392 [b], 654 [d]	398
	E_{pc} (mV)	279	294	304 [b], 578 [d]	324
	ΔE_{pa} (mV)	Nil	60	44	50
4	E_{pa} (mV)	371	424	402 [b], 664 [d]	390
	E_{pc} (mV)	279	307	290 [b,f]	294
	ΔE_{pa} (mV)	Nil	53	31	19

[a] All the experiments were carried out at a pH value of ca. 7 (no buffer).
[b] Relative to Fc^+/Fc.
[c] Relative to $Cu^{III/II}$ couple.
[d] Relative to $Ni^{III/II}$ couple.
[e] $\Delta E_{pa} = E_{pa,c} - E_{pa,f}$, error of E values, ± 3 mV.
[f] Irreversible.

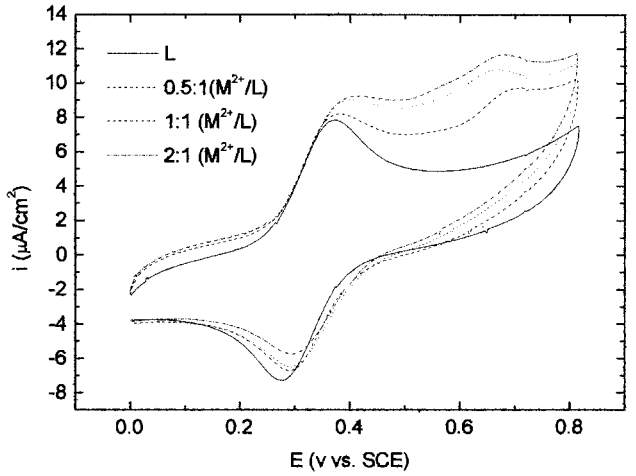

Fig. 5. Cyclic voltammograms of ligand **4** in the presence or absence of Ni^{2+}.

4. Conclusions

Cyclic voltammetry has revealed that Cu^{III} and Ni^{III} can be selectively stabilized by ligand **1** for Cu^{III} and by ligands **3** and **4** for Ni^{III}. Electronic absorption spectroscopy identified that the interaction between the ligands and the transition metal ions has an effect on the d-d transition of ferrocene and the guest cation. The complexation stoichiometry 1:1 (M^{2+}:L) for the complexes was verified by FAB MS results of the complexes and UV–vis titration. The equilibrium constants for the cobalt complex of **3** and **4** were evaluated.

Molecular systems capable of controlling the redox properties of metal ions are of interest in such fields as catalysis and electrocatalysis [7,14], in which some applications may be found on the basis of the electrochemical study results of these compounds.

Acknowledgements

We gratefully acknowledge the financial support from the National Natural Science Foundation of China. Peng Xue thanks Dr Zhong-xu Dai for helpful discussion about the electrochemical study. We feel in debt to Professor Fu-xing Gan of this University for the supply of electrochemical instruments.

References

[1] P.D. Beer, Adv. Inorg. Chem. 39 (1992) 79.
[2] G.W. Gokel, et al., Supramol. Chem. C371 (1992) 429.
[3] C.D. Hall, in: A. Togni, T. Hayashi (Eds.), Ferrocenes, VCH, Weinheim, 1995, pp. 279–316.
[4] A.E. Kaifer, S. Mendoza, in: G.W. Gokel (Ed.), Comprehensive Supramolecular Chemistry, vol. 1, Pergamon, Oxford, 1996, p. 701.
[5] M.J.L. Tendero, A. Benito, J. Cano, J.M. Lloris, R. Martinez-Manez, J. Soto, A.J. Edwards, P.R. Raithby, A. Rennie, J. Chem. Commun. (1995) 1643.
[6] (a) G. Oepen, F. Vögtle, Liebigs Ann. Chem. (1979) 1094. (b) R.M.T. Casey, P. Guinan, A. Canavan, M. McCann, C. Cardin, N.B. Kelly, Polyhedron 10 (1991) 483. (c) P.D. Beer, O. Kocian, R.J. Mortimer, P. Spencer, J. Chem. Soc. Chem. Commun. (1992) 602. (d) G.D. Santis, L. Fabrrizzi, Inorg. Chim. Acta 214 (1993) 193. (e) P.D. Beer, Z. Chen, M.G.B. Drew, J. Kingston, M. Ogden, P. Spencer, J. Chem. Soc. Chem. Commun. (1993) 1046. (f) P.D. Beer, J.E. Nation, S.L.W. McWhmme, M.E. Harman, M.B. Hursthouse, M.I. Ogden, A.H. White, J. Chem. Soc. Dalton Trans. (1991) 2485. (g) P.D. Beer, F. Szemes, J. Chem. Soc. Chem. Commun. (1995) 2245. (h) H. Bernard, J.J. Yaouanc, J.C. Clement, H. Des Abbayes, H. Handel, Tetrahedron Lett. 32 (1991) 369. (i) G.D. Santis, L. Fabrrizze, Inorg. Chem. 32 (1993) 854. (j) M.J.L. Tendero, A. Benito, R. Martinez-Manez, J. Soto, J. Paya, A.J. Edwards, P.R. Raithby, J. Chem. Soc. Dalton Trans. (1996) 343. (k) M.C. Grossel, D.G. Hamilton, P.N. Hotron, S. Neveu, R.A. Parker, P.S. Walker, Synthesis (1998) 78.
[7] (a) E. Fu, G. Wang, C. Wu, Syn. Commun. 28 (1998) 277. (b) P. Xue, E. Fu, G. Wang, C. Wu, Syn. Commun. 29 (1999) 1585.
[8] E. Kimura, in: S.R. Cooper (Ed.), Crown Compounds: Toward Future Application, VCH, Weinheim, 1992, p. 81.
[9] E. Kimura, J. Coord. Chem. 15 (1986) 1.
[10] L. Fabrizzi, F. Forlini, A. Perotti, B. Seghi, Inorg. Chem. 23 (1984) 807.
[11] (a) X. Bu, D. An, Z. Zhu, Y. Chen, M. Shionoya, E. Kimura, Polyhedron 16 (1997) 179. (b) X. Bu, Z. Zhang, D. An, Y. Chen, M. Shionoya, E. Kimura, Inorg. Chim. Acta 249 (1996) 125.
[12] R. Machida, E. Kimura, M. Kodama, Inorg. Chem. 22 (1983) 2055.
[13] H.A. Benisi, J.H. Hildebrand, J. Am. Chem. Soc. 91 (1949) 2703.
[14] M.F. Richardson, R.E. Sivers, J. Am. Chem. Soc. 94 (1972) 4134.
[15] L.L. Diaddari, W.R. Robinson, D.W. Margerum, Inorg. Chem. 22 (1983) 1021.
[16] (a) V.J. Thom, J.C.A. Boeyens, G.J. McDougall, R.D. Hancock. J. Am. Chem. Soc. 106 (1984) 3198. (b) T. Ito, K. Sugimoto, H. Ito, Chem. Lett. (1981) 1477.